Analysis of Interaction of Three Typhoons through 3-D Vorticity Tubess

Zhiying Ding, Song Gao, Xiaohui Zhao, Liguang Wu*
Key Disaster Laboratory of the Ministry of Education/Pacific Typhoon Research Center, NUIST, Nanjing,

1. INTRODUCTION

Strong vertical shear plays a very important role in forming and strengthening tornadoes and Supercell Storm. Davies-Jones (1980), through numerical experiments pointed that when the storm is moving, horizontal airflow rotation has something to do with the formation of upward current and downward current. Houze and Hobbs（1982）found that because there is the vertical shear of the horizontal wind, a horizontal axis vortex tube will be formed. After the upward current developed, the horizontal vortex tube rises. As a result, two vertical axis vortex tubes rotating in the opposite direction are formed. Because of the upward current uplifting, the above process also reflects the horizontal vortex tube gradually into a vertical vortex tube, ie, there is the conversion of horizontal vorticity to vertical vorticity. Mesoscale convective vortex formation is the result of both the convergence effect and the horizontal vorticity tilt effect (Skamarock et al., 1994; Davis and Weisman, 1994). At the beginning, the horizontal vorticity tilt effect that links to the level of buoyancy gradients caused by MCS has a role in making the vertical vorticity develop. Afterwards, the planetary vorticity of the middle troposphere strengthens the vertical vorticity (Zhu Aijun, Pan Yinong, 2007). Han Ying and Wu Rongsheng (2007), by studying the distribution of the Typhoon's horizontal vortex tube through different stages of development, put forward the conceptual model of the interaction between the spiral cloud zone, tangential wind and radial wind, and pointed out that due to the strong upward motion of the typhoon, horizontal vortex tube gradually transforms into vertical cyclonic vortex tube under the impact of the uplift of the vertical velocity, making the energy passed from the lower level to the high-level.

The studies of horizontal vorticity are often applied into the research of strong convection. The strong convection has strong vertical wind shear, which then becomes strong horizontal vorticity which transforms into vertical vorticity. It is well known that one of the conditions of the formation of a typhoon is that vertical shear becomes smaller, but outside the center of a typhoon, there is often a strong vertical wind shear. Will this vertical shear affects a larger scale typhoon? What is the relationship of horizontal vorticity and vertical vorticity during the occurrence of multi-typhoon? Can horizontal vorticity influence the typhoon circulation? What is the relationship of the interaction between horizontal vorticity and multi-typhoon? This paper will probe into these questions.

2. DATA AND METHODS

By using the data of NCEP / NCAR 1 ° × 1 ° analysis, and meso non-static WRF model 3.2.1 version, this thesis conducts the numerical simulation of the three typhoon process occurred from 00 a.m. August 3rd to 00 a.m. August 12th in 2009 in Western Pacific. The physical process and experiment scheme of the control experiment (CTRL) are as following:

(1) Use a triply two-way nested-grid. In the first grid the number of lattice is 96×86, the grid size is 45 km; in the second grid, the number of lattice is 129×78, the grid size is 15 km; in the third grid, the number of lattice is 96×86, the grid size is 5 km. The top of model is 50hPa, and the vertical layers are 27.

(2) Parameterization Scheme: cumulus convection parameterization scheme: the first and second grids are Kain/Fritsch scheme. The third grid doesn't use parameterization. Microphysical scheme used Lin et al. scheme. The long-wave radiation

* *Corresponding author address:* Prof. Zhiying Ding, Dept. of Atmospheric Sciences, Nanjing University of Information Science and Technology, Nanjing, MO 210044 email: Dingzhiying@nuist.edu.cn

scheme use rrtm scheme. The solar radiation scheme adopted Dudhia scheme.

Simulation time: 0000 UTC August 3rd— 0000 UTC August 8th, 2008

3. CONTRASTS OF THE ACTUAL SITUATION AND THE SIMULATION

In Figure 1, Goni's Northwest - Southwest - Southeast - Northeast circular track is basically simulated, but the track is to the east near Hainan Island. Morakot moves to the west, and changes its track to the northwest direction near Taiwan, and to the north after landing in Fujian, which has been largely consistent with the actual situation, except for only a slight westward deviation after landing in the mainland. Etau's track characteristics are also basically simulated. It first moves to the west, and then turns northward, and then into the eastward direction (northward moving is a little earlier than the actual situation).

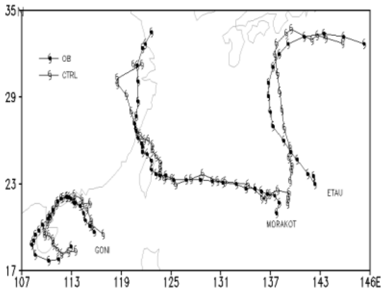

Fig.1. Comparison between the observed and control -run-simulated TC tracks at 6-hr intervals, with the initial time for Goni at 1200 UTC Aug.3, for Morakot at 1800, Aug.3 and for Etau at 1200, Aug.7, 2009 and the ending time for Goni at 1200, Aug.9, for Morakot at 1200, Aug. 11 and for Etau at 1800 UTC, Aug. 11, 2009.

It can be seen from Figure 2, the intensity and trends of Goni are both close to the actual situation. Only after 0000 UTC. 8th, the trends and intensity have deviation from the actual situation. The simulation doesn't simulate Goni's disappearance in the tropical ocean very well. Morakot's intensity and trend are close to the actual situation, but it is later for the simulation to reach maximum intensity than the actual situation does. The simulated strength of Etau has big deviation from the actual situation. It is related with its later formation, and the longer simulation time. It may also be related with the inadequate marine observational data and the inaccurate information of Etau's degree of strength. The simulation of the maximum wind speed near the center of the typhoon and the simulation results of the atmospheric pressure are quite consistent with the factual situation (Figure not shown). Simulations of Goni and Morakot are relatively better than that of Etau in track, intensity, and maximum wind speed.

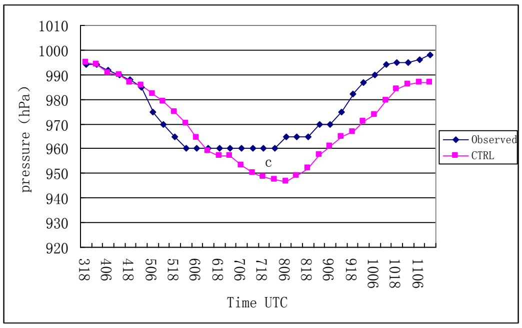

Fig.2 Time evolution of the central minimum mean sea level pressure of Morakot from JTWC (6-h interval) , and CTRL (6-h interval) from 1800 UTC 3 Jul to 1800 UTC 11 Aug 2009.

Overall, the controlled trial successfully simulates the three Typhoons process, and the results can be used for comparison and analysis.

4. THE HORIZONTAL VORTICITY IN TYPHOONS

Expression of the three-dimensional vorticity vector in the z coordinate system is as follows:

$$\zeta = \left(\frac{\partial w}{\partial y} - \frac{\partial v}{\partial z}\right)\vec{i} + \left(\frac{\partial u}{\partial z} - \frac{\partial w}{\partial x}\right)\vec{j} + \left(\frac{\partial v}{\partial x} - \frac{\partial u}{\partial y}\right)\vec{k}$$

It has been pointed out in previous studies that the atmospheric motion is mainly horizontal. Therefore, the influence of the vertical vorticity caused by the horizontal rotation on weather is very important. The statement holds on synoptic scale or large-scale conditions, and is accepted by people. By using magnitude analysis, in the horizontal direction, the vorticity w is fairly small, horizontal wind changes greatly with the increase of height. In the middle and lower troposphere, if there is lower-level jet wind, the vertical shear will reach 10^{-2}—$10^{-3}s^{-1}$, and it is the same near the jet wind. When the weather changes dramatically, generally there is a big vertical wind shear. The magnitude of vertical vorticity is generally 1-2 grades lower than that of the horizontal vorticity, which is similar to the relationship between vertical velocity and horizontal velocity, so for the typhoons, especially outside the center of the typhoon, a big horizontal vorticity should exist.

Figure 3a shows the contract of the actual NCEP 0.5 º × 0.5 º's horizontal vorticity value and the simulation in the 850 field at 00a.m. August 8, 2009. In the figure, there is a high horizontal vorticity value near the typhoon. The biggest value is up to $20\times10^{-3}s^{-1}$. How such a strong horizontal vorticity impacts the typhoon circulation deserves further attention.

It can also be seen in the figure the horizontal vorticity in Goni moving to Morakot, and the horizontal vorticity in the northern part of Morakot moving to Goni, whose strength is relatively smaller than that of the southern part of Goni moving to Morakot. The eastern part of Morakot also has a horizontal vorticity moving to the east into Etau. It can clearly be seen that Morakot, Goni and Etau interact with each other through the movement of horizontal vorticity. Morakot has a significant impact on Etau, while Etau has a smaller influence on Morakot through horizontal vorticity.

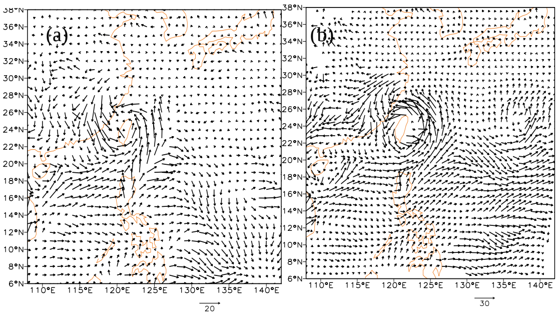

Fig.3 the 0000 UTC August 8th, 2009, 850hPa Observed (a) and forecasted (b) of horizontal vorticity ($10^{-3}s^{-1}$)

It can be seen from the contrast of the 0000 UTC August 8th 850hPa simulation of horizontal vorticity field and the actual field that the numerical simulation results of Goni and Morakot are very similar to the actual situation, but the simulation of Etau is still stronger than the actual situation.

It can be seen from the above analysis that the horizontal vorticities in the visible typhoons are very strong, and the simulation results are very close to the actual situation. Through the horizontal vorticities, interaction may exist between the typhoons, which needs further analysis.

In co-vector analysis of horizontal vorticity and vertical vorticity (Figure 4), there is a horizontal vorticity co-vector in the lower level under 900hPa. In around 900-800hPa, there is a horizontal vortex tube outflow, in 800-700hPa there is a vortex tube inflow. This is so in the typhoon evolution. The performance of the corresponding u, v component field shows a big wind speed value center under 850hPa. Above 700hPa, u, v component values reduce with height, and the three-dimensional vorticity vector mainly takes the form of divergence. If there are more centers on the vertical profile, the performance will show a multi-level vortex tube inflow. It can be seen in Figure 4a that the three-dimensional vortex tube of the typhoon has obvious mutual flow, a three-dimensional vortex tube outside of the middle and lower level of the typhoon moves eastward into another typhoon, and the three-dimensional vortex tube moves westward in the high-level, which may be related to the interaction of the typhoons.

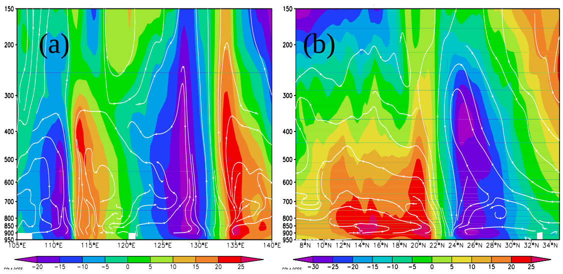

Fig.4 1200 UTC 5th along the 22.5ºN v-component (shaded) and the resultant vector of horizontal vorticity (x direction) and vertical vorticity profile (a) along the 132ºE u-component (shaded) and the resultant vector of horizontal vorticity (y direction) and vertical vorticity profile (b)

5. THE INTERACTION BETWEEN THE THREE TYPHOONS AND THE HORIZONTAL VORTICITY ADVECTION

Based on the analysis of the direction of typhoons' movement, the typhoon mainly moves to the west from 0600UTC 3rd to 1200UTC 7th. After 1200UTC 7th, it begins to move to the northwest. Five days later, from 850hPa diagram, it can be seen cloud water and rain water overlay diagram of the vicinity of 20.5 º N (Figure 5a), Goni's cloud band begins to flow toward Morakot. During the period, there are three phases, the first one is from the 5th to the 7th, the second 0000UTC the 7th to 1200 UTC the 8th, and the third is from 1200 UTC the 8th to 1200 UTC the 10th.

Especially in the second phase, there are flows from Morakot moveing to Goni. Therefore, these two typhoons interact with each other through the mutual cloud band transmission, while the formation and the cloud band transmission are related to the activity of vertical circulation, which has to do with horizontal vorticity, and horizontal vorticity advection.

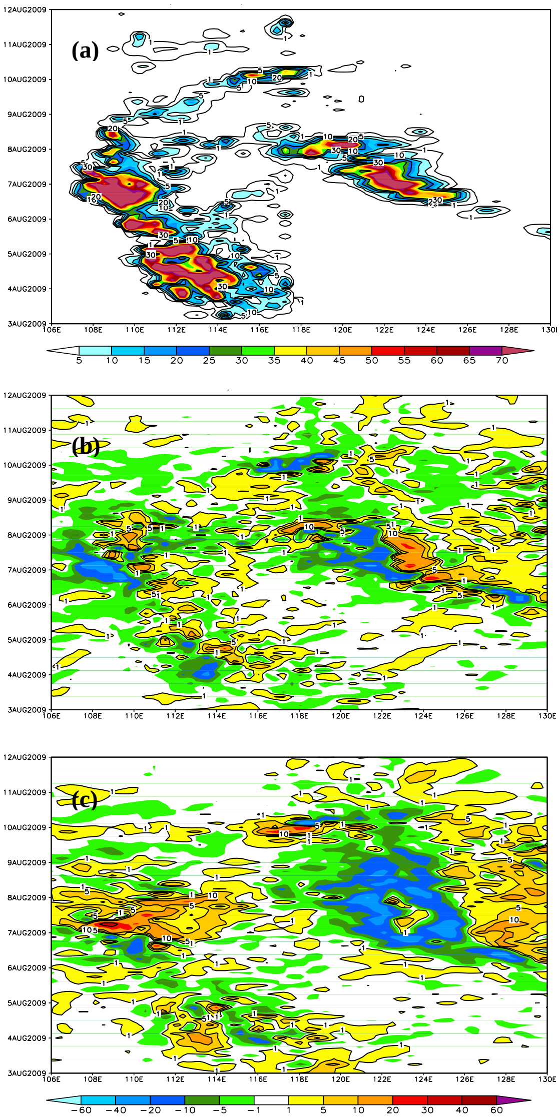

Fig.5 (a) Time evolution of cloud and rain water mixing ratio(g kg^{-1}),and (b)advection of horizontal vorticity (x direction) (c)advection of horizontal vorticity (y direction)from 1800 UTC 3 to 1800 UTC 12 Aug 2009 (interval :day) along 20.5° N，in 850hPa.

Figure 5b, and c shows that during the period of time when the interaction between cloud bands is quite strong, the horizontal vorticity also has large transmission, and the horizontal vorticity flowing along the x direction becomes strongest. Especially, at around 0000 UTC on the 8th a significant positive horizontal vorticity flows into the negative horizontal vorticity field of Morakot, which may lead to enhancing the cloud band in this region. Figure 6 shows cloud band often occurs in the region with high horizontal vorticity gradient. The activity of the cloud band between Morakot and Etau is not obvious, but it still shows the horizontal vorticity changes between the two typhoons and the weak cloud band activity.

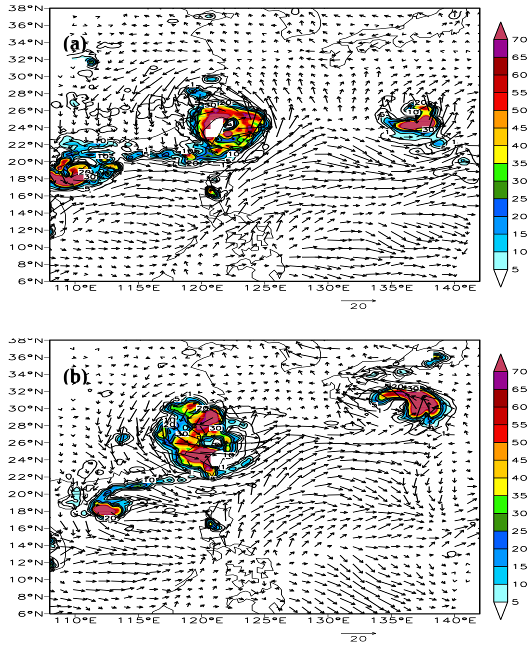

Fig. 6 850hPa, 0600 UTC 8th (a), 0900UTC 9th (b), the horizontal vorticity vector field and the cloud water, rain water mixing ratio(g kg^{-1})

From the 1200 UTC 6th, the 0000 UTC 7th, 850 hPa horizontal vorticity advection field distribution and wind field circulation(Figure 7), it can be seen that three typhoons are in the same monsoon low pressure, horizontal vorticity transmission occurs in the monsoon low pressure. The transmission can also be a manifestation of the interaction between typhoons.

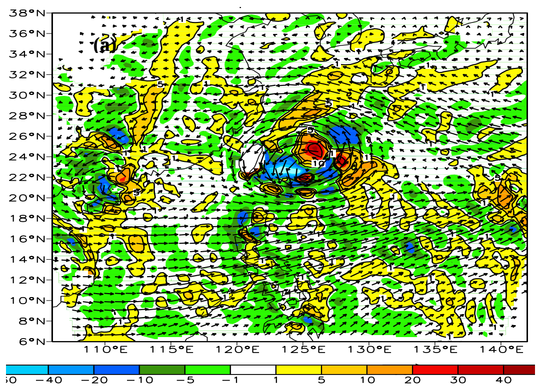

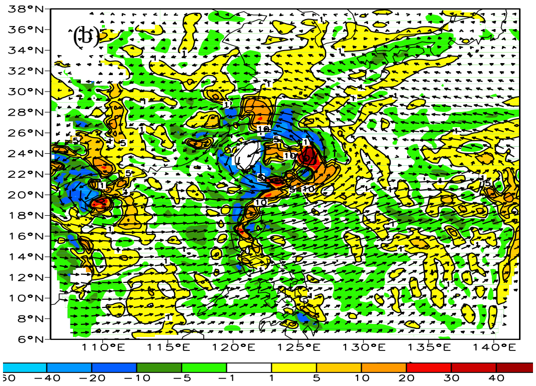

Fig.7 (a)850 hPa horizontal vorticity advection field（x direction , shaded, $10^{-8}s^{-1}$）and wind vector at 1200 UTC 6 Aug. ,(b) Same as Fig.7(a) but for 0000 UTC 7 Aug (y direcion)

6. CONVERSION OF TYPHOON'S HORIZONTAL VORTICITY TO VERTICAL VORTICITY

One of the key factors that can reflect the strength of the typhoon is wind speed. Vorticity is the rotation rate of the speed. The rotation rate in the horizontally direction is represented by the vertical vorticity. In the first section, the analysis shows that the horizontal vorticity value is big. It is by the conversion of the horizontal vorticity into vertical vorticity that typhoon wind speed increases, and affects the circulation of the typhoon.

By the vorticity equation that omits the friction item

$$\frac{\partial \zeta}{\partial t} = M + N + P + R + S ,$$

$$M = -[u\frac{\partial \zeta}{\partial x} + v(\beta + \frac{\partial \zeta}{\partial y})] ,$$

$$N = -\omega \frac{\partial \zeta}{\partial p} ,$$

$$P = -(\zeta + f)\nabla \cdot \vec{V} ,$$

$$R = -(\frac{\partial \omega}{\partial x}\frac{\partial v}{\partial p} - \frac{\partial \omega}{\partial y}\frac{\partial u}{\partial p}) .$$

In the above equation, M, N, P and R, are respectively the horizontal advection transmission, the vertical advection transmission, the horizontal convergence divergence and tilting. S refers to the friction, which is ignored in the following discussion. In the equation, u is the zonal horizontal wind speed, v is meridional horizontal wind speed, ω is vertical speed, ζ is vertical vorticity, f is the Coriolis parameter, $\beta = \frac{\partial f}{\partial y}$. W stands for the sum of the first four items. The tilting represents the conversion of the horizontal vorticity to the vertical vorticity, and this item is discussed as follows.

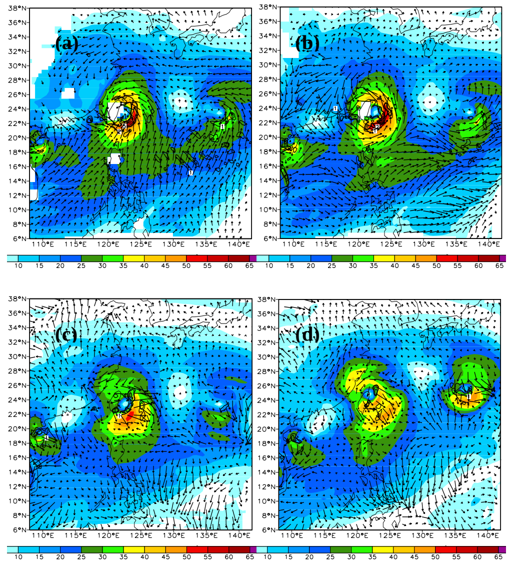

Fig. 8 1500 UTC August 7th, 900hPa wind speed (shadow, $m{\cdot}s^{-1}$) and tilting item (positive, unit: $\times10^{-8} \cdot s^{-1}$) vector is horizontal vorticity ($10^{-3} \cdot s^{-1}$).(b), (c)Same as Fig.8(a) but for 850hP, 700hPa, (d)Same as Fig.8(c) but for 1200 UTC August 8th

In the analysis of the three-dimensional distribution of the tilting item, in the vicinity of the typhoon center, above the 850hPa, the center of the tilting item's large value is outside the eye of the typhoon and the high wind speed center. As shown in Figure 6, in the 1500 UTC 7th, 900hPa map, the center of the maximum wind speed greater than $50ms^{-1}$ is located in the southeastern part of the typhoon center, and the center of the maximum wind speed greater than $2{\times}10^{-8}s^{-1}$ overlaps with the biggest center belt. This phenomenon continues until close to the typhoon's landing time. In the 850hPa map, the situation is basically the same, but the center of the maximum tilting item is quite messy. Around 700hPa, the positive value of the tilting item is obviously on both sides of the center of the maximum wind speed, and its value is relatively smaller than that of the lower level. Meanwhile, the direction of the vorticity vector shows great changes.

The direction changes from rotating cyclonically around the typhoon into mainly diverging from the center to the outside. The performance is more obvious in 200hPa. Under 850hPa, there is a conversion of the horizontal vorticity into the vertical vorticity near the maximum wind speed belt. This situation is conducive to the cyclonic circulation enhancements, which may lead to the increase of the typhoon lower level wind speed. With the increase of the height, the titling item tends to change on both sides of the largest center with the range of the growth of the cyclonic circulation and so it is conductive to the cyclonic circulation growth near the eye of the typhoon in the middle and high level, and to the cyclonic circulation increase outside of the lower level maximum wind speed. The titling item in the maximum wind speed center is negative, and the cyclonic circulation becomes weaker. This can be seen from the scope of the 700hPa >35m·s-1 wind field. This situation is most obvious in 700-600hPa, but the positive lower layer is small in scope and intensity. After the 00a.m. 8th, the strength of the anti-cyclonic circulation in the maximum wind speed belt increases, which may lead to the appearance of a new wind speed center outside the maximum wind speed (see Figure 6d).

In summary, in the maximum wind speed belt in the center of the typhoon, the lower tilting values are mainly positive, and the horizontal vorticity converts to the vertical vorticity, which has positive effects on the strengthening of the typhoon circulation, but has slight positive effects on both sides of the center of the maximum wind speed in about 700hPa. Near the center of the maximum wind speed, tilting values are mainly negative, which is detrimental to the development of cyclonic circulation.

7. SUMMARY

In conclusion, the results of the study are as follows:

(1) The distribution of the typhoon's horizontal vorticity is closely related to the distribution of the vertical wind field of the typhoon. In the case of the maximum wind speed, the horizontal vorticity convergence to the center of a typhoon goes along with the divergence. When there is the multi-center in the vertical direction, the forms of convergence and divergence are relatively complex.

(2) Horizontal vorticity mutual transmission exists in multi-typhoon, and three-dimensional vortex tube can get into another typhoon from the periphery of a typhoon. The activities of vortex tubes lead to the interaction of multi-typhoon.

(3) In the maximum wind speed belt in the center of the typhoon, the lower level tilting values are mainly positive, and the horizontal vorticity converts to the vertical vorticity, which has positive effects on the strengthening of the typhoon circulation, but has slight positive effects on both sides of the center of the maximum wind speed in about 700hPa. Near the center of the maximum wind speed, tilting values are mainly negative, which is detrimental to the development of cyclonic circulation.

Acknowledgments. This study is supported by National Key Basic Research Development Items Planning "973" (No. 2009CB421503), the Natural Science Foundation of China (40975037) .

References

Davies-Jones R P.1980 Tornado dynamics Thunderstorm: A Social and Technological Documentary. E. Kes-Ssler,Ed.

Davis C A, Weisman M L. Blanced dynamics of mesoscale vortices produced in simulated convective systems J Atmos Sci, 1994, 51(14): 2005-2030.

Han Y, Wu R S. On the Spiral Structure of Typhoon. J Nanjing Uni.（Natural Sciences）,2007，43(6)：572 -580.(in chinese)

Houze R A JR, Hobbs P V. 1982, Organization and structure of precipitating cloud systems. Advances in Geophysics , 24: 225-316.

Skamarock W C, Weisman M L, Klemp J B. 1994, Three-dimensional evolution of simulated long-lived squall lines. J Atmos Sci, 51(17): 2563-2584.